

Observation of proton-tagged, central (semi)exclusive production of high-mass lepton pairs in pp collisions at 13 TeV with the CMS-TOTEM Precision Proton Spectrometer

Pedro Duarte¹

¹Instituto Superior Tecnicos
University of Lisbon

Course on Physics at LHC

Introduction

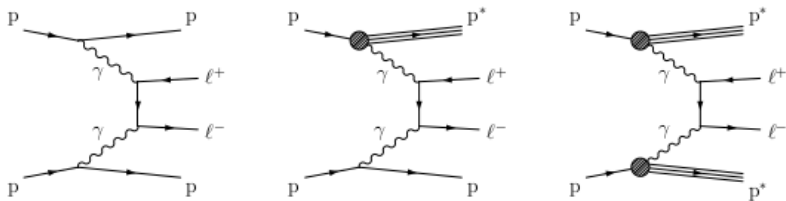


Figure: Exclusive (left), single proton dissociation or semiexclusive (middle), and double proton dissociation (right) topologies

Experimental Setup

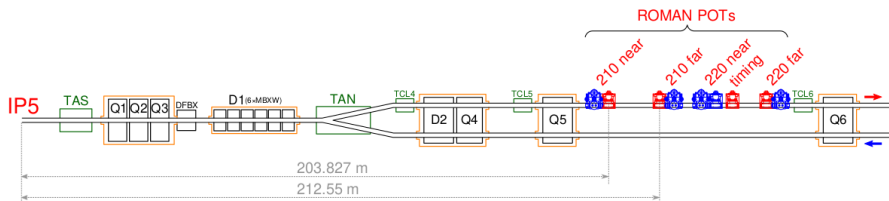


Figure: The layout of the beam line from the interaction point (IP) to the 210 m region on one of the arms of CT-PPS. Only detectors represented in red are part of the experiment. The blue ones are part of TOTEM.

Alignment of the CT-PPS detector

The alignment procedure consists of two conceptually distinct parts:

- Alignment in a special, low-luminosity calibration fill (alignment fill), where RPs are inserted very close to the beam.
- Transfer of the alignment information to the standard, high-luminosity physics fills.

Alignment of the CT-PPS detector - Alignment Fill

- Beam-based alignment - a procedure which takes place before data-taking and the purpose of which is to align the RPs with the LHC collimators and the beam.
- Relative alignment among RPs
- Absolute alignment - it is performed with a sample of elastic-scattering events tagged by the vertical RPs.

Alignment of the CT-PPS detector - Alignment Fill

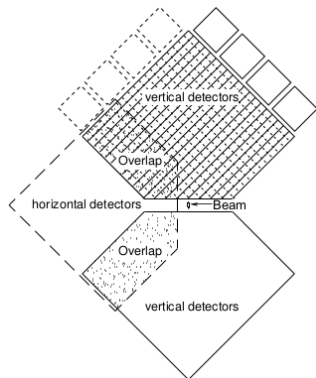


Figure: Schematic layout of the silicon strip detectors in one RP station

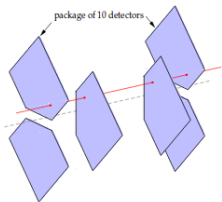


Figure: A track (red line) passing through an overlap between vertical and horizontal RPs. The blue areas represent stacks of 10 Si strip sensors. The dashed black line indicates the beam

Alignment of the CT-PPS detector - Physics Fill

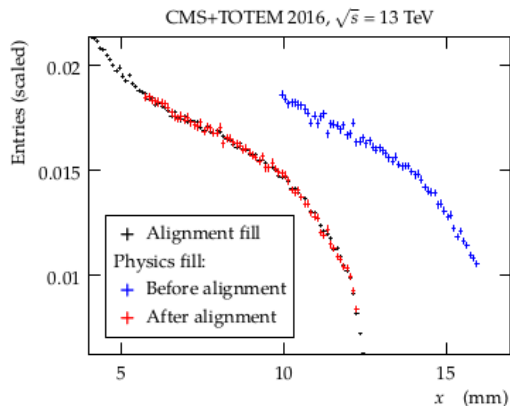


Figure: Illustration of the match metrics used for horizontal alignment. Black histogram: reference from the calibration fill. Blue (red) histogram: distribution from a physics fill before (after) matching.

Proton reconstruction - The LHC beam optics

The trajectory of protons is described by means of transport matrices $T(s, \xi)$, which transform the kinematics of protons scattered at the IP to the kinematics measured at the RP position

$$\mathbf{d}(s) = T(s, \xi) \mathbf{d}^* \quad (1)$$

, in which $d = (x, \Theta_x, y, \Theta_y, \xi)$, $\xi = \frac{\Delta p}{p}$, $x = D_x(\xi)\xi$, $y = L_y(\xi)\Theta_y^*$.
 The following approximations are also valid: $D_x \approx \frac{x_0}{\xi_0}$ and $x_0 \approx D_x \xi_0$.
 The index 0 represents any location s in the RP region, in which the value of ξ , ξ_0 , the factor L_y vanishes and the tracks concentrate around 0.

Proton reconstruction - The LHC beam optics

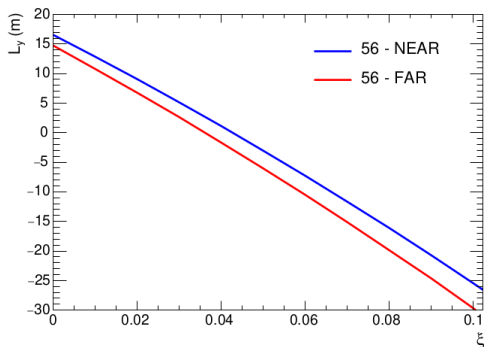


Figure: Vertical effective length L_y (in meters) as a function of the proton relative momentum loss at two (near and far) RPs

Proton reconstruction - Proton track reconstruction

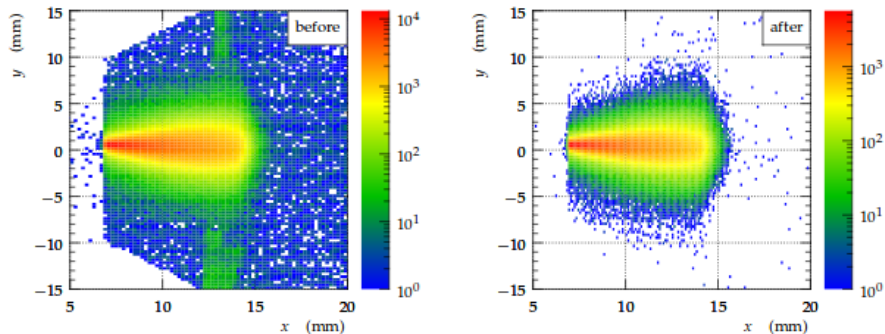


Figure: Distribution of the track impact points in the xy plane of one of the vertical Roman Pots (Beam position: $x=0$; $y=0$). Left: hit distribution before applying the cuts; Right: the same distribution after the cuts.

Proton reconstruction - Determination of ξ

ξ can be simply reconstructed by inverting Eq. (1). This method ignores subleading terms in the proton transport (notably the one proportional to the horizontal scattering angle); their effect is included in the systematic uncertainties. Other uncertainties include:

- Dispersion calibration: relative uncertainty in D_x of about 5.5 %.
- Horizontal alignment: corresponds an uncertainty of approximately $150 \mu\text{ m}$.
- The term Θ is neglected when the horizontal dispersion is estimated to be $D_x \approx \frac{x_0}{\xi_0}$.
- The subleading terms neglected in the approximations are also treated as systematic uncertainties.

Event selection- Central variables

- Events that are selected require the presence of at least two muon (electron) candidates of any charge, fitted to a common vertex, each with transverse momentum $p_T > 38(33)$ GeV.
- The invariant mass of the leptons is required to satisfy $m(l^+l^-) > 110$ GeV.
- In addition, the dilepton acoplanarity ($a = 1 - |\Delta\phi(l^+l^-)|/\pi$) is required to be consistent with the two leptons being back-to-back in azimuth ϕ .

Event selection- Central variables

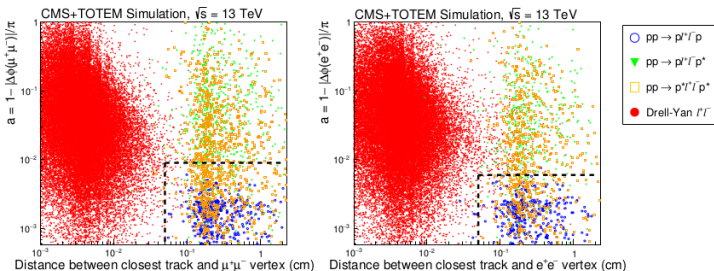


Figure: Dimuon (left) and dielectron (right) acoplanarity versus the distance between the closest extra track and the dilepton vertex for simulated signal and backgrounds.

Backgrounds

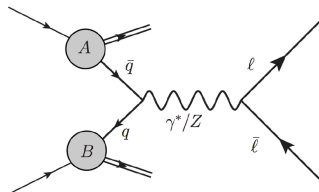


Figure: Drell-Yan Process

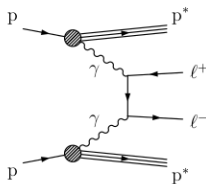


Figure: Double proton dissociation

Results - $\mu^+\mu^-$ Channel

- In the $\mu^+\mu^-$ channel, a total of 17 events were observed within the ξ acceptance of CT-PPS.
- No events are observed with matching protons in both arms.
- Highest mass event is at $m(\mu^+\mu^-) = 342$ GeV, 20 below the threshold for detection in both arms.

Results - e^+e^- Channel

- In the e^+e^- channel, a total of 23 events were observed within the ξ acceptance of CT-PPS.
- No events are observed with matching protons in both arms.
- Highest mass events are at $m(e^+e^-) = 650$ GeV and at $m(e^+e^-) = 917$ GeV, in the region where the double-arm acceptance is nonzero.

Results

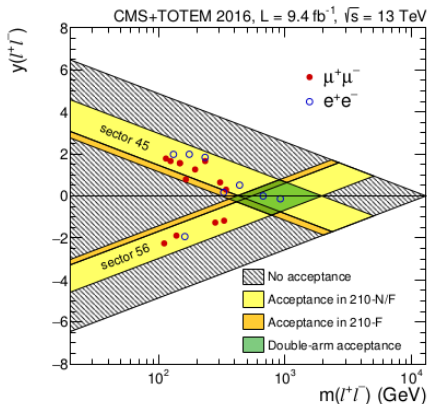


Figure: Expected acceptance regions in the rapidity vs. invariant mass plane overlaid with the observed dimuon (closed circles) and dielectron (open circles) signal candidate events